Asian Journal of Scientific Research

ISSN 1992-1454

science alert
http://www.scialert.net

ANSInet
an open access publisher
http://ansinet.com

Asian Journal of Scientific Research 1 (6): 562-578, 2008
ISSN 1992-1454

Heat Transfer Enhancement in the Presence of an Electric Field at Low and Intermediate Reynolds Numbers

E. Esmaeilzadeh, A. Alamgholilou, H. Mirzaie and M. Ashna
Department of Mechanical Engineering,
University of Tabriz, Tabriz, 51666-14766, Iran

Abstract: The aim of this study is an application of the EHD actuator on local heat transfer enhancement by using wire-plate electrodes in laminar and turbulent duct flow. In this study, the effects of an electric field and temperature field on the fluid flow as an active method of enhancement is numerically investigated. The hydrodynamics and heat transfer behaviors of laminar and turbulent duct flow with specific boundary conditions in the presence of an EHD actuator was taken into consideration. The partial difference equations of flow field and electric field namely continuity, momentum and energy equations for fluid flow and electric current and Poisson's equations for electric field was numerically solved with finite volume method. At first, the electric equations were solved and then the results were imported to the fluid field for improvement of the body forces. The obtained results show for the flows with Re≤1000 with single wire-plate electrode is suitable for local enhancement. By adding the number of wires to three, it is possible to use this method for turbulent flow up to Re = 2000.

Key words: Duct flow, heat transfer, enhancement, EHD, corona wind

INTRODUCTION

If a high voltage electric field applies between a thin wire and conductor plate, the dielectric fluid in surrounding will be affected by ions injection from wire. These ions move towards the plate electrode and impact with neutral fluid molecules and change their momentum. This phenomenon creates a secondary flow in cross wise of the main flow in duct and affects its heat transfer rate.

The EHD actuator classifies as active methods of heat transfer enhancement. It has several advantages: It is noiseless, low power consumption and easily controllable, applicability in complex geometries and etc.

The enhancement effect will be augmented by increasing the applied voltage. The electrical breakdown strength of fluid must be known and should not exceed. Poor design may result in electrical breakdown, which make the EHD actuator system useless (Solymar and Walsh, 1988; Mohsseni, 1998).

Marco and Velkoff (1963) for first time used corona wind as an active method of heat transfer enhancement. They used this method in natural convection of a vertical plate with constant heat flux and could enhance the mean value of heat transfer rate up to five times as much.

Yabe and Hijikata (1978) in an experimental and numerical study determined the pressure and density of ions over a horizontal surface of a receiver containing dry nitrogen. They could be able to recognize the recirculation region of the fluid caused by corona wind provided by a wire-plate actuator. Also the enhancement of heat transfer in the zone of stagnation point of impingement jet of corona wind over the plate with constant temperature has been minutely obtained.

Corresponding Author: Esmaeil Esmaeilzadeh, Department of Mechanical Engineering, University of Tabriz, Tabriz, 51666-14766, Iran Tel: 0098-4113393054, 09141160374 Fax: 0098-4113354153

Ohadi *et al*. (1991) used the wire-plate electrodes for forced convection enhancement in pipe flow. They showed that the two-wire electrode design provided a modestly higher enhancement than did the single wire electrode design. With two electrodes, they showed that for Reynolds numbers up to 10000, it is possible to use this technique for enhancement.

Allen and Karayanis (1995) and Seyed-Yagobi and Bryan (1999) published the review papers for enhancement of heat transfer and mass transport in single-phase and two-phase flows with electrohydrodynamics. They showed the importance of this method in vast application.

Owsenek *et al*. (1995) investigated the experimental study of corona wind heat transfer enhancement with a heated horizontal flat plate. They enhanced the heat transfer rate significantly by the application of corona wind between corona needle and ground plate by introducing a jet impingement facility of corona needle and high voltage power supply more than 25 times of natural convection.

Seyed-Yagobi and Owsenek (1997) investigated the theoretical and experimental works on EHD heat transfer enhancement through wire-plate corona discharge in air flow over a horizontal surface with constant heat flux.

Ohadi *et al*. (2003) compared a numerical model of EHD-enhanced heat transfer in air laminar channel flow with experimental results. The main contribution of their study is to implementation of corona wind in a duct with small hydraulic diameter. This kind of geometry is of great interest in compact heat exchangers.

Yamamoto *et al*. (2003) investigated the three-dimensional electric field and space charge density distributions and the flow interaction between the primary flow and secondary flow (EHD flow). From the simulation, they showed that for better understanding of the particle motion and collection efficiency equation in the industrial ESP's, the EHD actuators could be applied as a convenient device.

Zhao and Adamiak (2005) investigated numerically the effect of airflow, including the EHD flow produced by the electric corona discharge and the flow generated externally on the corona discharge. They solved numerically the equations for the electric field, charge transport and fluid flow simultaneously. In their work a numerical algorithm was presented for the numerical simulation of the effects of secondary EHD flow and the external airflow on the electric corona discharge in the pin-plate and the pin-mesh configuration. They showed that the EHD flow produced by the electric corona discharge has a negligible effect on the corona discharge. But the effect of the external air flow on the corona discharge depends on the air velocity and the configuration of the system and this can be much stronger.

Fujishima *et al*. (2006) provided the flow interaction between the primary flow and the secondary flow in the wire-duct electrostatic precipitator. They extended to incorporate the alternately oriented point corona on the wire-plate type electrodes. Their study was extended to include the turbulent flow model for alternately oriented spiked-electrode, which leads to further understanding of the detailed flow interaction in the industrial ESP's.

Chun *et al*. (2007) performed numerical calculation to solve the 2D flow of a turbulent low/high Reynolds number for investigation of EHD flow by using the single wire-plate actuators. They studied particularly the wake downstream near the corona wire. Furthermore, the mechanisms of EHD secondary flow for turbulent flow were modeled by the Chen-Kim modified $k-\varepsilon$ turbulent model.

The momentum and energy equations are coupled through the temperature dependence of the permittivity and thermal conductivity of the fluid. So, it is noted that analytical solution of the EHD coupled momentum and energy equations is not possible (Ahmadi *et al*., 2004). But fortunately in air flow applications because of negligible term of Joule heating in energy equation, the problem becomes uncoupled. Hence, in this study the heat transfer enhancement of laminar and low Reynolds turbulent flows in duct has been numerically investigated for uncoupled field. For the laminar case the single wire-plate can enhance the cooling effect but for intermediate Reynolds turbulent flow the triple wire-plate has been used for convenience.

THEORETICAL APPROACH AND GOVERNING EQUATIONS

It is assumed that the material properties are constants and the corona is directed from wire to the plate, since this corona wind is generally stable. Neglecting the end effects in rectangular cross section of duct, a two-dimensional electrohydrodynamic model can be assumed. The analysis of the flow behavior with electric field can be done by numerical solution of the corresponding governing equations for steady, incompressible EHD flows.

The governing equations of both fields are:

- Gauss's law:

$$\nabla^2 V_e = -\frac{\rho_e}{\beta} \tag{1}$$

- Conservation of charge:

$$\vec{\nabla}.(V_e\rho_e) = \vec{\nabla}.(D\vec{\nabla}\rho_e) + b\vec{\nabla}.(\rho_e\vec{\nabla}V_e) = 0 \tag{2}$$

- Electric field or electrical potential relation:

$$\vec{E} = -\vec{\nabla}V_e \tag{3}$$

- Conservation of electric current

$$\vec{\nabla}.\vec{J} = 0 \tag{4}$$

$$\vec{J} = \rho_e.b.\vec{E} \tag{5}$$

By substitution of $\vec{J}$ in Eq. 4 the final case of conservation of electric current becomes:

$$\beta_0.\vec{E}.\nabla\rho_e = -\rho_e^{\,2} \tag{6}$$

In Eq. 1-6, V_e is electrical potential, ρ_e is the charge density, D is the ion diffusivity in gas, b is the mobility, $\vec{E}$ is electric field intensity vector, β is the permittivity of the medium and $\vec{J}$ is the electric current.

- Continuity for gas flow:

$$\vec{\nabla}.\vec{u} = 0 \tag{7}$$

- Conservation of momentum:

$$\vec{u}.\vec{\nabla}\vec{u} = -\frac{1}{\rho}\vec{\nabla}P + \nu\nabla^2\vec{u} + \rho_e\vec{E} \tag{8}$$

- Energy equation:

$$\vec{\nabla}(\rho\vec{u}c_p T) = \vec{\nabla}.(K\vec{\nabla}T) + b\rho_e\vec{E}^2 \tag{9}$$

In this study the mobility of ions in air is about $b = 10^{-6}\ m^2\ V^{-1}\ s^{-1}$ so in Eq. 9 the joule heating term ($b\rho_e\vec{E}^2$) becomes negligible. In Eq. 7-9, $\vec{u}$ is air flow velocity vector, ρ is fluid density, P is the fluid pressure, ν is fluid kinematics viscosity, T is the fluid temperature, c_p is specific heat of fluid at constant pressure and K is thermal conductivity of fluid.

Equation 1-9 show that, in general, the electrical potential, the charge density, the gas velocity and the gas temperature are coupled. These coupled systems of equations for some simple cases can be solved numerically (Ahmadi *et al*., 2004). However in our study, as it mentioned, the Joule heating term in Eq. 9 is negligible and in Eq. 8 the last term of Coulomb force ($\rho_e\vec{E}$) is the only influence of electric field in the fluid field. Hence, we assumed the equations are uncoupled for iterative solution of problem. At first we solve numerically the electric equations independent from the fluid equations and then from the results we improve the body force in Eq. 8 by replacing the values of Coulomb force as a source term in momentum equations.

For Reynolds numbers over 1000, obviously the flow in duct is turbulent. The effects of EHD in this kind of applications are concentrated to the low and moderate Reynolds numbers. Hence for present case the Reynolds number is limited to 2000. The k−ε standard turbulence model was provided (Warsi, 2006):

- k Equation:

$$\bar{u}_j\frac{\partial k}{\partial x_j} = P - \varepsilon + \frac{\partial}{\partial x_j}\left(\frac{\nu_T}{\sigma_k}\frac{\partial k}{\partial x_j}\right) + \nu\nabla^2 k \tag{10}$$

Where:

$$\nu_T = 0.09\frac{k^2}{\varepsilon}$$

- ε Equation:

$$\bar{u}_j\frac{\partial \varepsilon}{\partial x_k}\left(C_\varepsilon\frac{k}{\varepsilon}\bar{\tau}_{kl}\frac{\partial \varepsilon}{\partial x_l}\right) + C_{\varepsilon 1}\frac{\varepsilon P}{k} = -C_{\varepsilon 2}f_\varepsilon(R_T)\frac{\varepsilon}{k}\left[\varepsilon - 2\nu\left(\frac{\partial\sqrt{k}}{\partial n}\right)^2\right] + \nu C_{\varepsilon 3}\bar{\tau}_{ij}\frac{k}{\varepsilon}\frac{\partial^2\bar{u}_k}{\partial x_i\partial x_l}\frac{\partial^2\bar{u}_k}{\partial x_j\partial x_l} + \nu\nabla^2\varepsilon \tag{11}$$

Where:

$f_\varepsilon(R_T) = 1 - \frac{2}{9}\exp(-R_T^2/36)$

$R_T = K^2\nu\varepsilon$

$C_\varepsilon = 0.15$

$C_{\varepsilon 1} = 1.44$

$C_{\varepsilon 2} = 1.92$

$C_{\varepsilon 3} = 2$

NUMERICAL PROCEDURE AND BOUNDARY CONDITIONS

Equation 1 and 6 for electric field are discritized in the standard form of the finite volume method by using the upwind scheme. As it seen in Eq. 2 there are 2 terms in the conservation of charge. The 1st term is diffusion of ions in media and the 2nd term is the ions mobility term. In this case the 1st term is negligible in comparison with the 2nd one. So, the Eq. 2 becomes:

$$\nabla(\rho_e b\vec{E}) = 0 \tag{12}$$

In this condition charges move only downward through electric field. So, if we discrete the domain of solution, the movement of ions is only in the longitudinal direction. Therefore it is rational to use the upwind scheme in discretization of electric field equations. For fluid flow SIMPLE algorithm and Hybrid scheme are applied for numerical procedure.

DUCT GEOMETRY AND THE BOUNDARY CONDITIONS

Figure 1 shows the schematic of the solution domain. The test duct is 1000 mm length, 200 mm height; the distance of wire from upper surface of duct has 3 values which will be mentioned in discussion of the results. Wire to inlet domain is 320 mm, wire to outlet domain is 680 mm and its diameter is 4 mm.

For the geometry shown in Fig. 1 the following electric boundary conditions are used:

Along a (inlet condition):

$$\frac{\partial \rho_e}{\partial x} = 0, \frac{\partial E}{\partial x} = 0 \tag{13}$$

Along b (outlet condition):

$$\frac{\partial \rho_e}{\partial x} = 0, \frac{\partial E}{\partial x} = 0 \tag{14}$$

Along wire surface:

$$E = E_0 \tag{15}$$

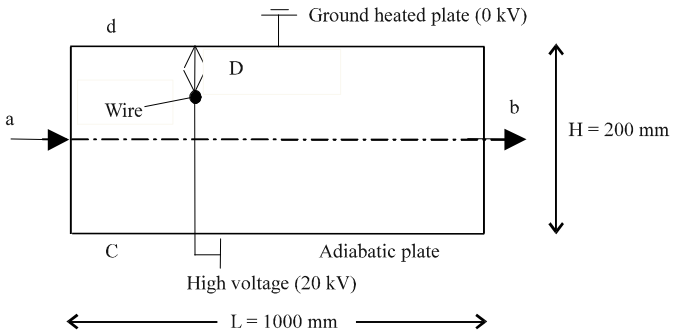

Fig. 1: Schematic geometry of main problem

For wire surface charge density, a method of try and error iteration is used. In first step, a primitive value for ρ_e is guessed then the electric current from wire to plate is calculated. From the assumption has been used by a large number of authors in past (Takimoto *et al*., 1988; Allen and Karayannis, 1995; Zhao and Adamiak, 2005) and for prevention of breakdown phenomenon in dielectric media, it is recommended to limit the intensely of electric current around μA to few mA. In the next steps the values of ρ_e are corrected.

In the recent study of Ahmadi *et al*. (2004) based on the Peek's formula of the onset of electric field strength (Peek, 1929), for coronation of wire they use:

$$\vec{n}.\vec{\nabla}E = E_{onset} \tag{16}$$

where, $\vec{n}$ is the local unit normal vector that points into the wire, $\vec{\nabla}E$ is the gradient of voltage on the wire and E_{onset} is the electric field threshold strength for corona onset. E_{onset} is calculated with Peek's formula for an iterative procedure applying the charge density condition on the wire.

Along c (lower surface of duct):

$$\frac{\partial E}{\partial x} = 0, \frac{\partial E}{\partial y} = 0 \tag{17}$$

Along d (upper surface of duct, ground electric):

$$E = 0 \tag{18}$$

For the flow of air in domain we have:

Along a:

$$u = U_0, v = 0, T = T_0$$

Along b:

$$\frac{\partial u}{\partial x} = 0$$

Along wire surface:

$$u = 0, \; v = 0$$

Along c:

$$u = 0, \; v = 0, \; \frac{\partial T}{\partial y} = 0$$

Along d:

$$u = 0, \; v = 0, \; T = T_d$$

The main purpose of this study is the cooling of upper heated surface with constant temperature by the air flow in presence of an EHD corona wind. Hence, the previous boundary conditions for the flow and heat transfer have been considered.

RESULTS AND DISCUSSION

The air flow is laminar and moderate turbulent Reynolds numbers which are extended up to 2000. The Reynolds number is based on height of channel. With attention to the height of channel is half of

hydraulically diameter, the flow in channel will be not laminar. Iulet temperature $T_0 = 273°C$, upper surface temperature of duct $T_d = 300°C$ and constant physical properties of air as: $\rho = 1.225$ kg m^{-3}, $C_p = 1007$ J kg^{-1} K^{-1} and Pr = 0.71. Applied voltage is in the range of 5 to 20 kV. In the case of turbulent flow, the intensity of the inlet values of k and ε are often unknown and the advice is to take guidance from experimental data for similar flows. The simplest practice is to assume uniform values of k and ε computed from (Kim, 1990):

$$k = (IU_0)^2, \varepsilon = (C_\mu C_d)^{0.75}\frac{k^{1.5}}{0.1H} \tag{19}$$

where, I is the turbulent intensity (typically in the range $0.01<I<0.05$), U_0 is iulet mean velocity and H is a characteristic inlet dimension, say the height of the duct. The inlet conditions for k and ε of duct flow based on Eq. 19 has been taken $k_0 = 1.4\times10^{-5}$, $\varepsilon_0 = 4\times10^{-7}$. In the numerical procedure, the mesh is refined and its final size independence for solution has been gained for 250 cells in stream wise and 35 cells in crosswise direction. In beginning, for validation and the accuracy of the calculation, we used an especial geometry which is shown in Fig. 2. From this geometry, we were able to compare our results with the experimental PIV pictures of Jerzy *et al*. (2004).

In this case the intensity of electric current remains between 400 to 500 μA. The applied voltage was 24 kV from wire to plates. Mean inlet air velocity of fluid is 0.2 m sec^{-1} and Reynolds number is about 2000. Therefore this Reynolds number is a little more than the case of laminar flow; it is required to introduce for flow field a turbulence model with moderate intensity of turbulence in flow. We used the standard k-ε model and solved the momentum equations coupled with electric field. Figure 3 shows our numerical results for velocity vector distribution in domain. The result obtained by Jerzy *et al*. (2004) from their numerical procedures and experimental works has been taken for comparison in this study. The boundary conditions in all of these results are the same. Their experimental work was taken by an image of flow visualization which was obtained by PIV method (Fig. 4). The results are fairly agreement between them.

For 1st study case, the Reynolds number is extended from 100 to 1000, therefore it remains laminar in these cases. Then for low Reynolds turbulent cases we extend the work up to 2000.

Table 1 shows the distances of wire from upper surface (D) and applied voltage, the electric current calculated by iteration in fluid medium for the case of laminar flow in which we use ouly single wire plate.

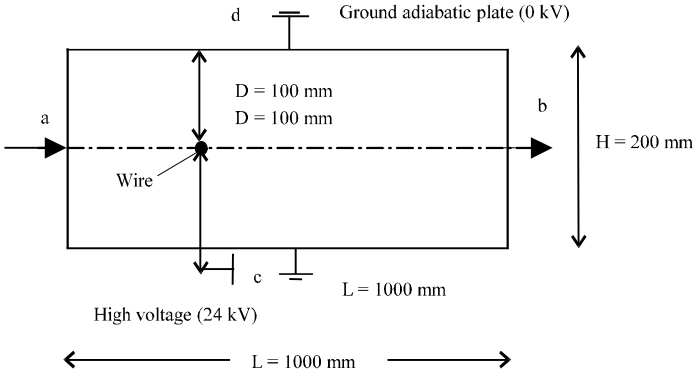

Fig. 2: Geometry of domain for comparison with Jerzy *et al*. (2004)

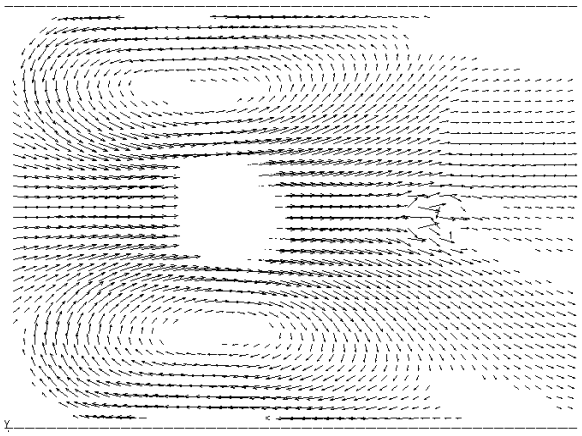

Fig. 3: Velocity vectors in this study

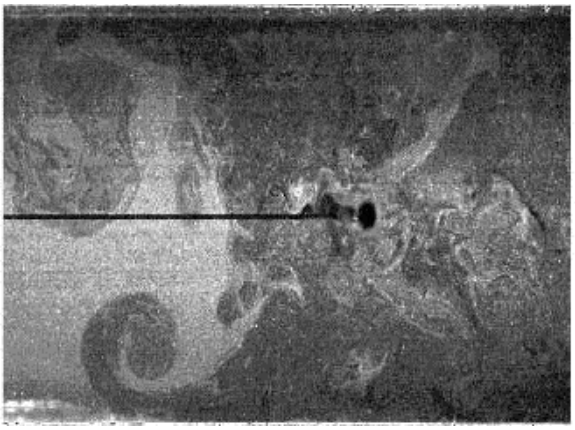

Fig. 4: PIV picture of flow field (Jerzy *et al*., 2004)

Table 1: Electric current values obtained by iteration method

Electric current (kV)	D = 48 mm	D = 60 mm	D = 72 mm
5	I = 117 μA	I = 90 μA	I = 60 μA
10	I = 260 μA	I = 200 μA	I = 140 μA
15	I = 402 μA	I = 309 μA	I = 250 μA
20	I = 642 μA	I = 495 μA	I = 400 μA

For the case of Reynolds over 1000, we use three wire electrodes in the transverse direction of flow with only 20 kV applied voltage. In Fig. 5 the schematic arrangements of wire electrodes is shown.

Figure 6 shows potential distribution of voltage in the streamwise and crosswise direction of flow in duct. These graphs has been plotted from the computed results for 20 kV applied voltage between electrodes and D = 60 mm. In Fig. 6b as it is seen the potential voltage did not approach to zero value

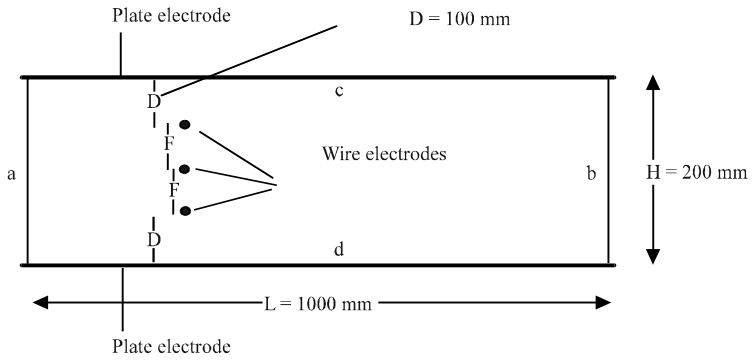

Fig. 5: Schematic geometry of main problem for turbulent flow

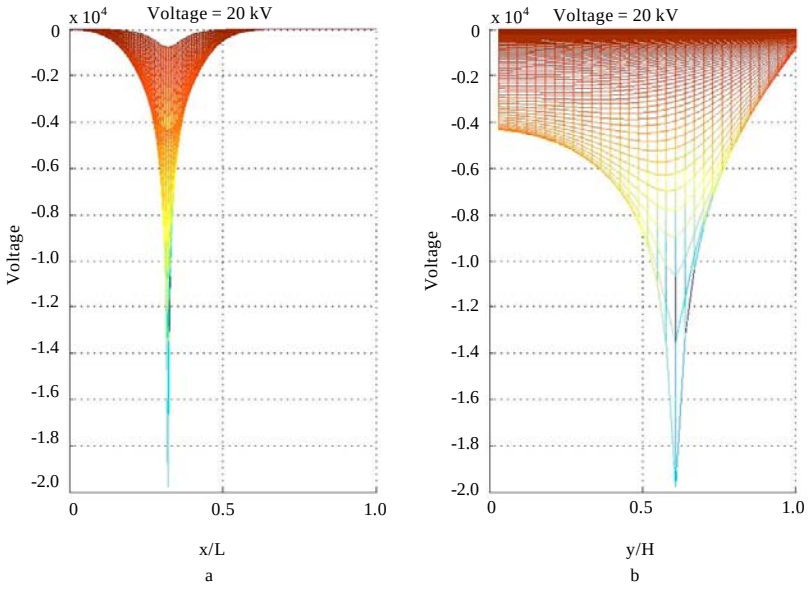

Fig. 6: Voltage distribution for single wire plate with D = 60 mm; (a) Longitudinal and (b) Lateral

for lower plate of channel. The reason of this phenomenon is the electrically insulated case of lower plates. In comparison of Fig. 6a and b, it is obviously shown the strong effect of corona wind is in crosswise direction of flow.

Figure 7 shows potential distribution of voltage in the case of triple wires with the plates of channels as cathode electrodes in streamwise and crosswise direction of flow in duct. These graphs has been plotted from the computed results for 20 kV applied voltage between electrodes and D = 46 mm. In all of the figures as it is seen the potential voltage distributions is symmetric. In comparison of Fig. 7a and b, it is obviously shown the strong effect of corona wind in crosswise direction. It is clear that for this case, the effects of corona wind caused by stronger electric fields become more effective than the previous case. Hence it can be used for heat transfer enhancement as an effective active tool for moderate Reynolds numbers.

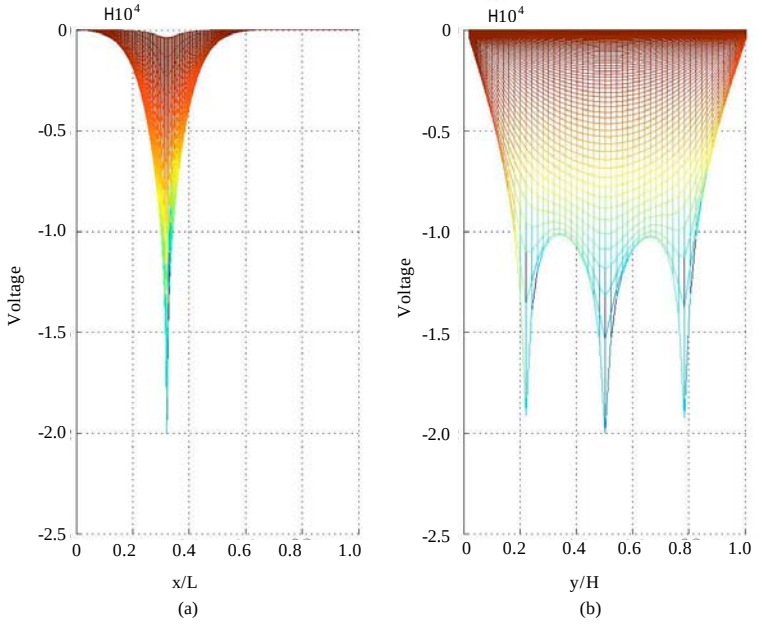

Fig. 7: Voltage distribution for triple wire plate with D = 46 mm; (a) Longitudinal and (b) Lateral

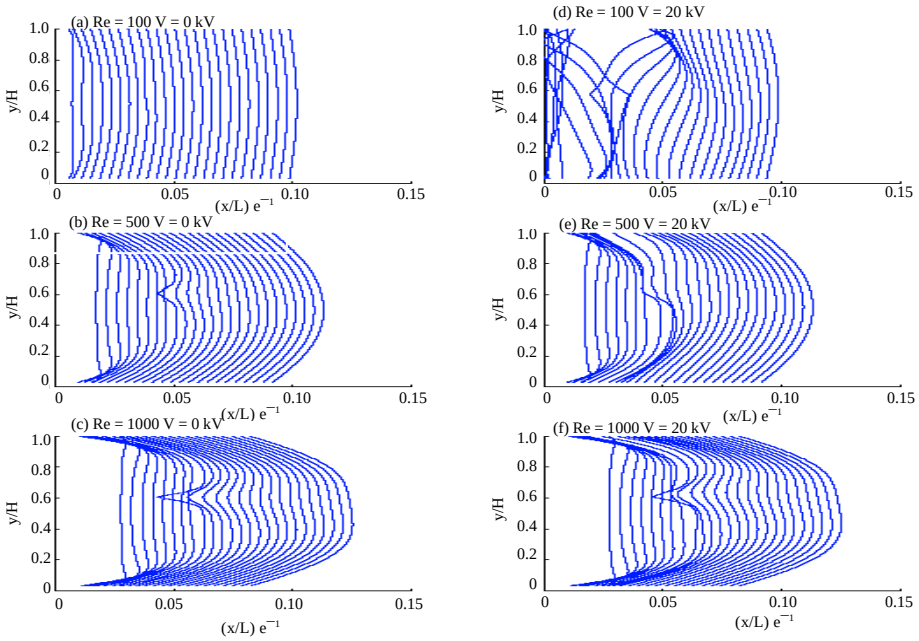

Fig. 8: Comparison of the velocity profiles

Results for Laminar Flow

Figure 8 shows the velocity profiles in both cases of non electric fields and applying 20 kV for D = 60 mm and 3 Reynolds numbers 100, 500 and 1000.

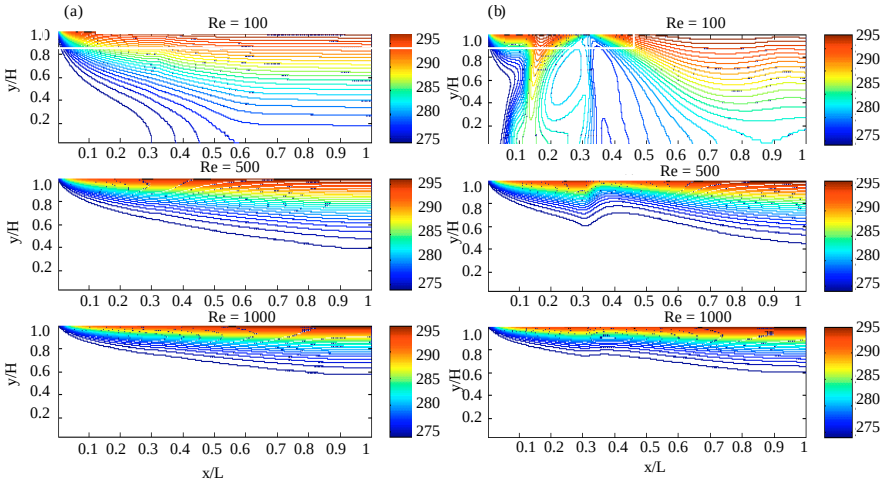

Fig. 9: Comparison of the temperature contours in two cases; (a) Without applied voltage and (b) With applied voltage (20 kV)

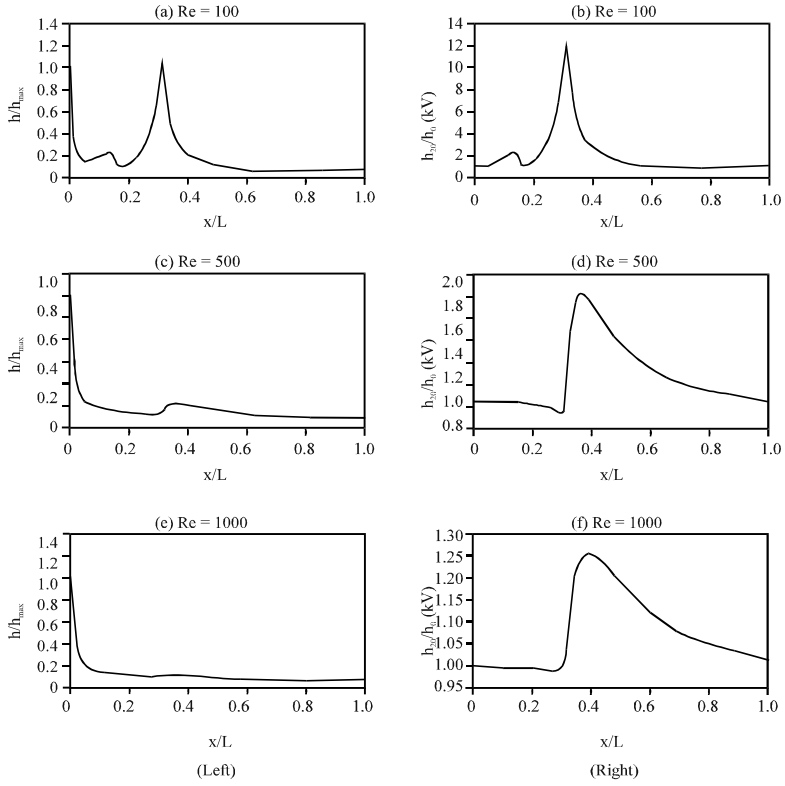

Fig. 10: Heat transfer coefficient ratio versus x/L for Reynolds 100, 500 and 1000 (Left) h_{20}/h_{max}, (Right) h_{20}/h_0

As it is seen, the local effects of the secondary flow caused by corona wind are manifested in the velocity profiles closed to the electrodes. The distortion of profiles becomes significant for low Reynolds numbers. In Fig. 8, for the same conditions, the temperature contours are depicted. As it is illustrated, for low Reynolds numbers from the secondary flow of EHD, the distortions of temperature field are intensively affected around electrodes.

In Fig. 9 for the same conditions as before, the temperature contours are depicted. As it is shown, for low Reynolds numbers from the secondary flow of EHD, the distortions of temperature field are intensively affected around electrodes.

In Fig. 10 the heat transfer coefficients illustrated in two manners. In left column, the curves of a, c and e (left) represent h/h_{max} versus x/l. Where h_{max} is the maximum value of h just in the beginning section of domain. In second way, the curves b, d and f (right) which are plotted for h_{20}/h_0 versus x/l. Wherein h_0 is the heat transfer coefficient without corona wind and h_{20} with 20 kV applied voltage. As it seen, for low Reynolds numbers, h locally increased and extended downstream. The heat transfer coefficient h, enhanced above ten times more than that of h_0. It is also mentioned, the enhancement for Re = 100 becomes 10 times of Re = 1000.

For other applied voltages, similar result was achieved. It is obvious, for high voltage and small distances of wire to plate, the enhancement is important.

In Fig. 11a-c, the ratio of h/h_0 (h with EHD and h_0 without it) are plotted versus Reynolds numbers. The applied voltage was in the range of 5 to 20 kV and the distance of wire to upper plate has been taken for 3 values of 48, 60 and 72 mm. As it is shown by increasing Reynolds numbers and decreasing applied voltages, the enhancement of heat transfer decreases for all of electrode distances.

From Fig. 12 the variation of h_{20}/h_0 versus D/H becomes nearly linear. In all cases of investigations, the slop of variation for low Reynolds numbers is steeper than others.

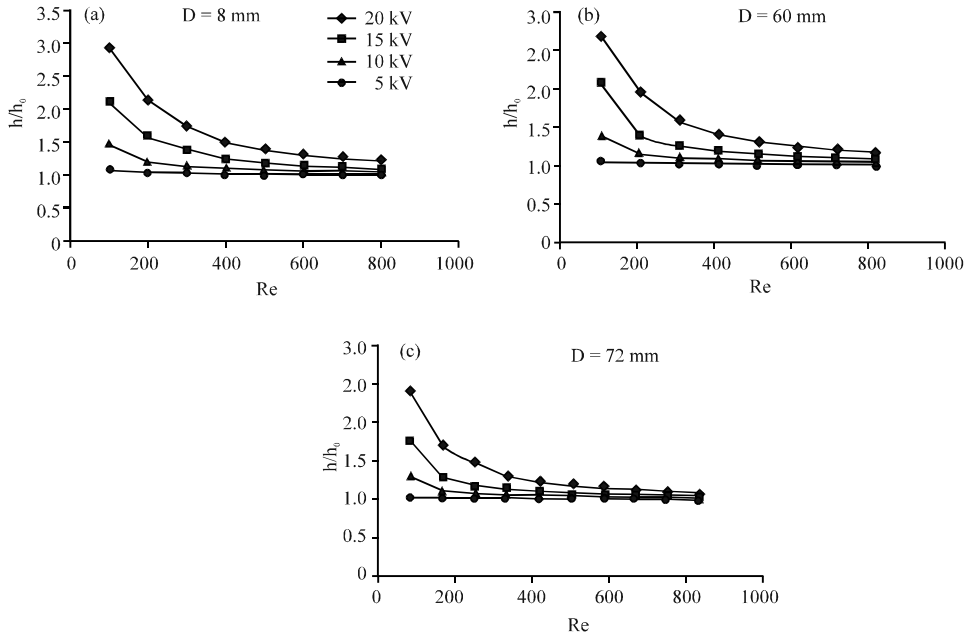

Fig. 11: Variation of h/h_{20} versus Re for 5 kV ≤ V ≤ 20 kV and D = 48, 60 and 72 mm

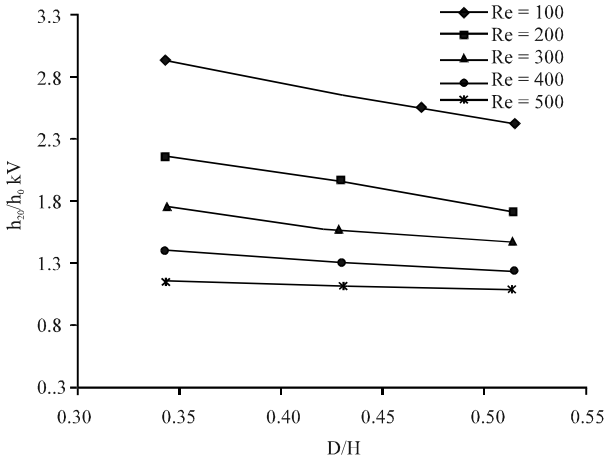

Fig. 12: Effect of distance D on enhancement of heat transfer for diverse Re and 20 kV voltage

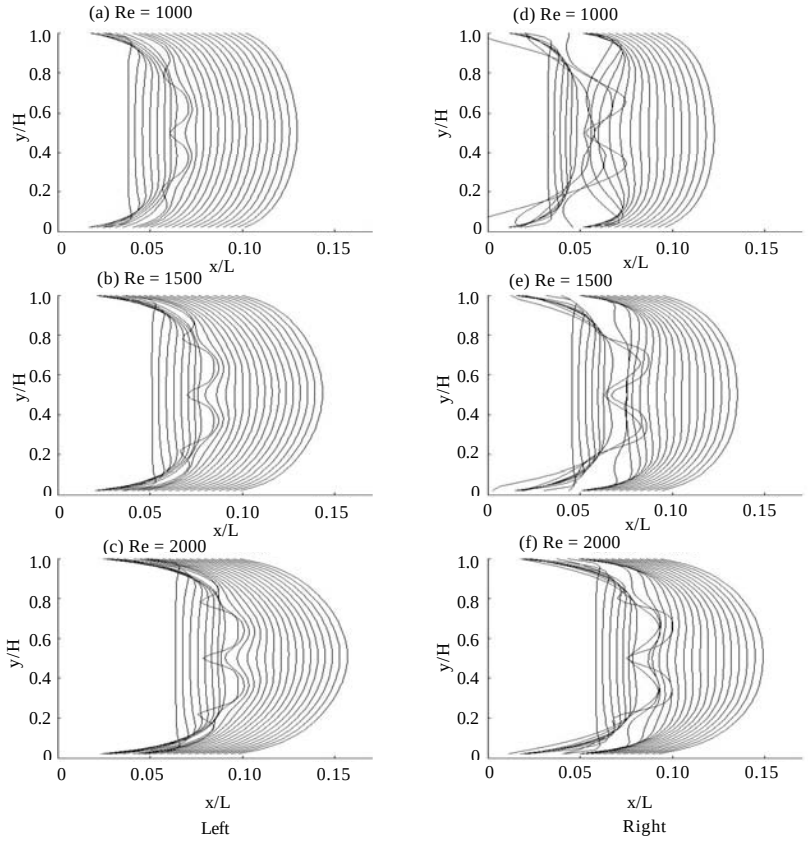

Fig. 13: Longitudinal and lateral distribution of velocity with triple wires; (Left) without electric field and (Right) with electric field

Results for Turbulent Flow

Figure 13 shows the streamwise and crosswise velocity distributions in both cases of non electric fields and applying 20 kV for D = 46 mm and three Reynolds numbers 1000, 1500 and 2000.

The triple wires as cathode and upper and lower plates of duct as anode is arranged in Fig. 5. From these results, as it is shown the presence of three wires in flow field without EHD actuator has small effects on momentum transfer and is concentrated in the vicinity of wires. When the corona winds of EHD actuator is initiated, deformations of profiles in both directions become important. Therefore augmentation of momentum transfer caused by secondary flows of corona could transport excess enthalpy. Then, the active enhancement of heat transfer occurred.

From Fig. 14 the effects of corona winds on temperature distribution near upper wall is clearly demonstrated. As it is seen for Reynolds 1000, cooling of the heated plate is more effective than the higher Reynolds. This fact was proved earlier by interpretation of momentum transfer in Fig. 13.

In Fig. 15 the curves of a, c and e are presented for the heat transfer coefficients of h/h_{max} versus x/l. Where h_{max} is the maximum value of h just in the beginning section of domain. The curves of b, d and f (right) which are plotted for h_{20}/h_0 versus x/l shown the comparison of corona effects on heat transfer enhancement. Wherein h_0 is heat transfer coefficient without corona wind and h_{20} with 20 kV applied voltage. As it is seen, triple wires-plates actuator has enhancement role even up to 2000 Reynolds numbers. In comparison between Fig. 10 and 15 for the case of Re = 1000 it is seen that using three wire-plate electrodes instead of single wire-plate electrode could increase mean heat transfer enhancement from 25 to 35%.

In Fig. 16, the maximum values of augmentation of heat transfer versus Reynolds numbers are shown.

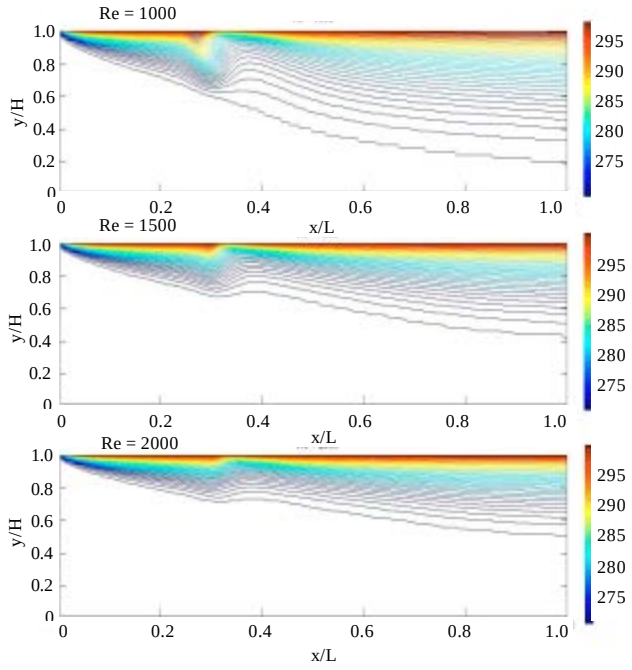

Fig. 14: Temperature distributions with applied voltage triple wires plates (20 kV), For Re = 1000, 1500 and 2000

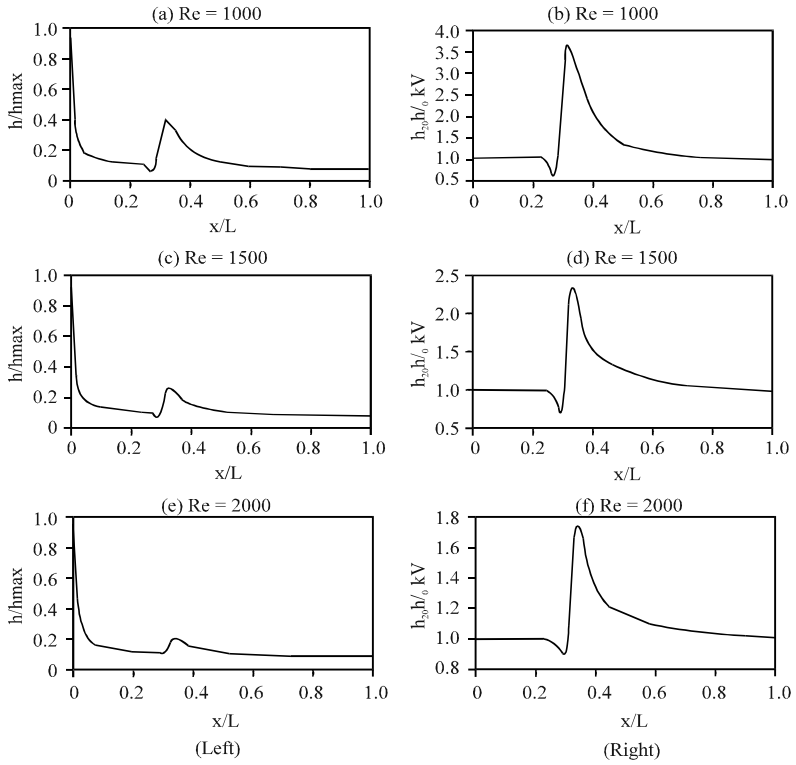

Fig. 15: Heat transfer coefficient ratio versus x/L for Reynolds 1000, 1500 and 2000 (Left: h_{20}/h_{max}, Right: h_{20}/h_0)

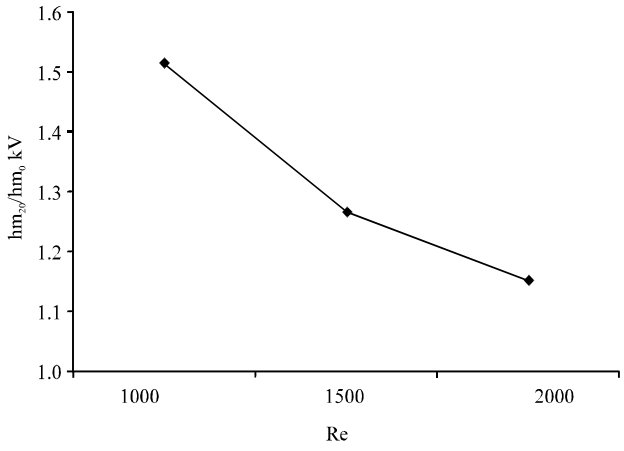

Fig. 16: Heat transfer enhancement versus Reynolds number

In Fig. 17 the performance evaluation criteria of the active enhancement technique of EHD in duct for low and intermediate Reynolds numbers are shown. Single wire plate actuator has significant effects in laminar duct flow (Re<1000). As it is seen by decreasing the distance of wire to plate, enhancement

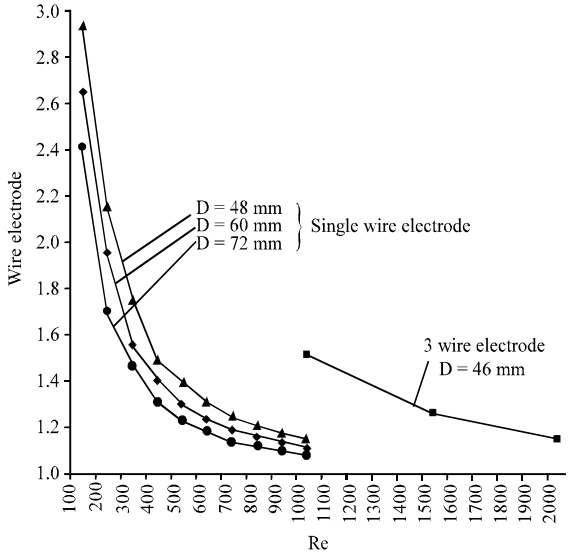

Fig. 17: Performance Evaluation Criteria for EHD actuators for Reynolds numbers up to 2000

phenomenon is increased. For Reynolds numbers higher than 1000 this method is ineffective. Hence, for Reynolds numbers up to 2000, the triple wire-plate actuator should be applied in order to gain desired enhancement.

CONCLUSION

The ability of our calculation code based on finite volume method is proven for prediction of an active method of heat transfer enhancement by using EHD phenomenon in duct flow. The results for local and mean values of heat transfer enhancement in laminar duct flow up to 1000 Reynolds numbers, show that the single wire-plate electrodes is suitable. For Reynolds numbers from 1000 up to 2000 using triple wire-plate actuator could be effective. For single wire-plate actuator, low Reynolds numbers, high voltage and short distance of wire to plate have more local effects on enhancement. For Re = 100, D = 48 mm and V = 20 kV the mean heat transfer enhancement reaches near 200%. This value decreases to below 25% for Re = 1000. In using of triple wire-plate actuator for the same Reynolds number the value increases 2 times and even more. In turbulent flow for Re = 2000, applying triple wire-plate actuator could provide 20% of enhancement.

ACKNOWLEDGMENT

This study has been supported by grant No.39/2239 of the Research Council Department of the University of Tabriz.

REFERENCES

Ahmadi, G., P. Zamankhan and F. Fa-Gung, 2004. Coupling effects of the flow and electric fields in electrostatic precipitators. J. Applied Phys., 96: 7002-7010.

Allen, P.H.G. and T.G. Karayannis, 1995. Electrohydrodynamic enhancement of heat transfer and fluid flow. Heat Recovery Syst. CHP., 15: 389-423.

Chun, Y.N., J.S. Chang, A.A. Berezin and J. Mizeraczyk, 2007. Numerical modeling of near corona wire electrohydrodynamic flow in a wire-plate electrostatic precipitator. IEEE. Trans. Dielectrics Elect. Insulation, 14: 119-124.

Fujishima, H., Y. Morita, M. Okubo and T. Yamamoto, 2006. Numerical simulation of 3D electrohydrodynamics of spiked-electrode electrostatic precipitators. IEEE Trans. Dielectrics Elect. Insulation, 13: 160-167.

Jerzy, M. *et al*., 2004. Measurements of the velocity field of the flue gas flow in an electrostatic precipitator model using PIV method. J. Comput. Phys., 193: 697-707.

Kim, S.W., 1990. Near-wall turbulence model and its application to fully-developed turbulent channel and pipe flows. Numer. Heat Transfer, 17: 101-122.

Marco, S.M. and H.R. Velkoff, 1963. Effect of electrostatic fields on free convective heat transfer from heat plates, ASME Paper No. 63. HT. 9, pp: 63-72. http://www.emeraldinsight.com/Insight/ViewContentServlet?Filename=Published/EmeraldFullTextArticle/Pdf/1340140301_ref.html.

Mohsseni, H., 1998. Advanced Electrical High Voltage Engineering. 5th Edn. Tehran University Press, Tehran, Iran, ISBN 4-4029-03-964.

Ohadi, M. *et al*., 1991. Heat transfer enhancement of laminar and turbulent pipe flow via corona discharge. Int. J. Heat Mass Transfer, 34: 1175-1178.

Ohadi, M., A. Shooshtari and F.H.R. Franca, 2003. Experimental and numerical analysis of electrohydrodynamic enhancement of heat transfer in air laminar channel flow. Semiconductor Thermal Measurement and Management Symposium, 19th Annual IEEE, March 11-13, IEEE Xplore, London, pp: 48-52.

Owsenek, B.L., J. Seyed-Yagoobi and R.H. Page 1995. Experimental investigation of corona wind heat transfer enhancement with a heated horizontal flat plate. J. Heat Transfer, 117: 309-315.

Peek, W., 1929. Dielectric Phenomenon in High Voltage Engineering. 1st Edn. McGrawHill, New York, ISBN 1-55937-160-9.

Seyed-Yagoobi, J. and B.L. Owsenesk, 1997. Theoretical and experimental study of EHD heat transfer enhancement through wire-plate corona discharge. J. Heat Transfer ASME, 19: 604-610.

Seyed-Yagoobi, J. and J.E. Bryan, 1999. Enhancement of heat transfer and mass transport in single-phase and two-phase flows with EHD. Adv. Heat Transfer, 33: 95-104.

Solymar, L. and D. Walsh, 1988. Lectures on the Electrical Properties of Materials. 1st Edn. Oxford University Press, London, ISBN-0-19-856192-X.

Warsi, Z.U.A., 2006. Fluid Dynamics; Theoretical and Computational Approaches. 3rd Edn., Taylor and Francis, New York, ISBN 0-8493-3397-0.

Yabe, A. and K. Hijikata, 1978. EHD study of the corona wind between wire and plate electrodes. AIAA J., 16: 340-345.

Yamamoto, T., M. Okuda and M. Okubo, 2003. Three-dimensioual ionic wind and electrohydrodynamics of tuft/point corona electrostatic precipitator. Ind. Applied IEEE Trans., 39: 1602-1607.

Zhao, L. and K. Adamiak, 2005. Effects of EHD and external air flows on electric corona discharge in pin-plate configuration. Industry Applications Conference, 14th IAS Annual Meeting, Conference Record of the 2005, Oct. 2-6, IEEE Xplore, London, pp: 2584-2589.